Acta Pharmaceutica Sinica B 2017;7(2):167–172

Chinese Pharmaceutical Association
Institute of Materia Medica, Chinese Academy of Medical Sciences

Acta Pharmaceutica Sinica B

www.elsevier.com/locate/apsb
www.sciencedirect.com

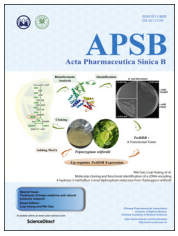

ORIGINAL ARTICLE

A set of interesting sequoiatones stereoisomers from a wetland soil-derived fungus *Talaromyces flavus*

Tianyu Sun[a], Jian Zou[a], Guodong Chen[a,*], Dan Hu[a], Bin Wu[b], Xingzhong Liu[b], Xinsheng Yao[a], Hao Gao[a,*]

[a]*Institute of Traditional Chinese Medicine and Natural Products, College of Pharmacy, Jinan University, Guangzhou 510632, China*
[b]*State Key Laboratory of Mycology, Institute of Microbiology, Chinese Academy of Sciences, Beijing 100190, China*

Received 7 May 2016; revised 22 June 2016; accepted 27 June 2016

KEY WORDS

Wetland soil-derived fungus;
Talaromyces flavus;
Stereoisomers;
Sequoiatone;
Electronic circular dichroism

Abstract Four interesting sequoiatones stereoisomers (**1**–**4**) were isolated from a wetland soil-derived fungus *Talaromyces flavus* by chiral HPLC. On the basis of comprehensive NMR and mass analyses, their planar structures were elucidated as the same as that of sequoiatone B. Among them, **1** and **3** (or **2** and **4**) were a pair of enantiomers, and **1** and **2** (or **3** and **4**) were a pair of stereoisomers with epimerization at C-12, which indicated that sequoiatione-type metabolites exist as enantiomers rather than as optically pure compounds in some strains. With the quantum chemical ECD calculations, the absolute configurations of C-8 in **1**–**4** were determined, which is the first report to establish the absolute configuration of C-8 in sequoiatones. However, the absolute configurations of C-12 in sequoiatones are still unsolved.

*Corresponding authors. Tel.:/fax: +86 20 85228369.
E-mail addresses: chgdtong@163.com (Guodong Chen), tghao@jnu.edu.cn (Hao Gao).

Peer review under responsibility of Institute of Materia Medica, Chinese Academy of Medical Sciences and Chinese Pharmaceutical Association.

http://dx.doi.org/10.1016/j.apsb.2016.07.005

1. Introduction

Sequoiatones, a kind of fungal metabolites, possess an octahydrocyclopenta[*c*]pyran skeleton with a long conjugated system[1–3], which is similar to the azaphilones monascorubrin and monochaetin[4,5]. To date, only few sequoiatones, such as sequoiatones A-F, were isolated from fungi *Aspergillus parasiticus* and *Penicillium* sp.[1–3], and their structural diversity depend on diversiform ring systems (dicyclic or tricyclic systems), the position of CH_3 in pyran ring (at C-5 or C-6), the unsaturation of olefin (C-6–C-7), and the hydroxylation at C-18.

In the course of our search for bioactive secondary metabolites from wetland fungi[6–10], the chemical investigation of metabolites from *Talaromyces flavus* (AHK07-3) was carried out, which led to the isolation of four stereoisomers (**1**–**4**) (Fig. 1) of sequoiatones with chiral HPLC (Fig. 2), whose planar structures were the same as that of sequoiatone B. According to the analyses of NMR, optical rotation, and electronic circular dichroism (ECD) data, **1** and **3** (or **2** and **4**) were a pair of enantiomers, and **1** and **2** (or **3** and **4**) were a pair of stereoisomers with epimerization at C-12. In addition, the absolute configurations of C-8 in **1**–**4** were determined by quantum chemical ECD calculations. Detail of the isolation and structural elucidations of compounds **1**–**4** are presented herein.

2. Results and discussion

Compound **1** was obtained as a yellow oil. The quasi-molecular ion at *m/z* 375.2177 $[M+H]^+$ by HR-ESI-MS indicated the molecular formula of **1** was $C_{22}H_{30}O_5$ with 8 degrees of unsaturation. The ^{13}C NMR spectrum combined with the DEPT-135 spectrum showed 22 signals (Table 1), assigned to seven sp^2 quaternary carbons [including one ketone carbonyl (δ_C 208.0), one ester carbonyl (δ_C 165.4), and five olefinic carbons (δ_C 168.7, 163.9, 152.7, 135.4 and 106.7)], three sp^2 methine carbons (δ_C 141.9, 113.2 and 106.6), one sp^3 oxygenated quaternary carbon (δ_C 77.7), one sp^3 methine carbon (δ_C 47.4), five sp^3 methylene carbons (δ_C 34.0, 31.7, 29.4, 27.4 and 22.6), and five methyl carbons (δ_C 50.9, 27.3, 20.3, 17.4 and 14.1). In the ^1H NMR spectrum of **1** (Table 1), the characteristic signals of one exchangeable proton [δ_H 7.54 (1H, s)], three aromatic or olefinic protons [δ_H 7.40 (1H, s), 7.21 (1H, s) and 6.96 (1H, s)], one sp^3 methine proton [δ_H 2.67 (1H, m)], and five methyl protons [δ_H 3.84 (3H, s), 2.26 (3H, s), 1.53 (3H, s), 1.14 (3H, d, J=6.9 Hz) and 0.86 (3H, t, J=6.8 Hz)] were observed. The non-exchangeable proton resonances were associated with the directly attached carbon atoms in the HSQC experiment (Table 1). The analysis of the ^1H–^1H COSY experiment and the coupling values of the protons indicated the presence of one subunit (C-22–C-12–C-13–C-14–C-15–C-16–C-17–C-18) as shown in Fig. 3. Combined with the above deduced subunit and molecular formula, the HMBC correlations from H_3-18 to C-16/C-17, from H_3-19 to C-1, from H_3-20 to C-4/C-5, from H_3-21 to C-7/C-8/C-9, from H_3-22 to C-11/C-12/C-13, from H-4 to C-5/C-7/C-20, from H-6 to C-3/C-5/C-7, from H-10 to C-2/C-8/C-9/C-11, from 8-OH to C-7/C-8, and the NOESY correlations between H_3-19 and H-4/H-10, revealed the planer structure of **1** (Fig. 3). The assignments of all proton and carbon resonances are provided in Table 1. Furthermore, the key NOESY correlation between H_3-19 and H-10 also suggested the *Z* configuration of the trisubstituted olefin (C-9–C-10) in **1**.

Compounds **2**–**4** were also obtained as yellow oils. Based on the analysis of HR-ESI-MS data, the molecular formulas of **2**–**4** were the same as **1**. Furthermore, the 1D and 2D NMR data revealed that **2**–**4** had the same planer structure as **1**, which were stereoisomers of **1**. In addition, the irradiation of H_3-19 causing enhancements of H-10 in the selective 1D NOESY experiment of **2**–**4** revealed the *Z* configurations of the trisubstituted olefin (C-9–C-10) in **2**–**4**, which were the same as **1** (see Supplementary Information Figs. S14, S21 and S27).

In the structures of **1**–**4**, there are two stereogenic centers (C-8 and C-12) in the skeleton, which are isolated by three carbons. Detailed analyses of the 1D NMR data of **1**–**4** presented that the NMR data of **1** and **3** are identical except for the exchangeable proton (Table 1). The similar observation was in NMR data of **2** and **4**, and there is only 0.01 ppm offset at H_b-13. Two sets of NMR data with little offset (0.01/0.1 ppm) at few protons/carbons (except for exchangeable protons) can be recognized as identical[11]. For the identical NMR data and the similar absolute values of optical rotations but in opposite directions of **1** and **3** (or **2** and **4**), **1** and **3** (or **2** and **4**) should be a pair of enantiomers.

Between **1** and **2** (or **3** and **4**), there were several noticeable offsets at C-10 (0.2 ppm), H-12 (0.02 ppm), and C-22 (0.3 ppm)/H_3-22 (0.02 ppm) (Table 1), which resulted from the epimerization at C-8 or C-12. In ECD experiments, the ECD curves of **1** and **2** were similar with each other, which were opposite to those of **3** and **4**. To investigate the effect of different configurations of C-8 and C-12 to ECD of **1**–**4**, the ECD calculations were carried out. Since the flexible side chain at C-12 has negligible effect on the ECD of **1**–**4**, the simplified structures (8*S*,12*R*)-**5**, (8*R*,12*S*)-**5**, (8*R*,12*R*)-**5**, and (8*S*,12*S*)-**5** were used for ECD calculations[12–16]. The calculations (Fig. 4) showed that the signs of major cotton effects of these structures were apparently controlled by the absolute configuration of C-8. The experimental data of **1** and **2** were similar to the predicted ECD curve of (8*R*,12*R*)-**5** (Fig. 5), which suggested that the absolute configurations of C-8 in **1** and **2** were *R*. The experimental data of **3** and **4** were similar to the predicted ECD curve of (8*S*,12*R*)-**5** (Fig. 5), which suggested that the absolute configurations of C-8 in **3** and **4** were *S*. Therefore, the epimerization between **1** and **2** (or **3** and **4**) was at C-12. However, the configurations of C-12 were not determined.

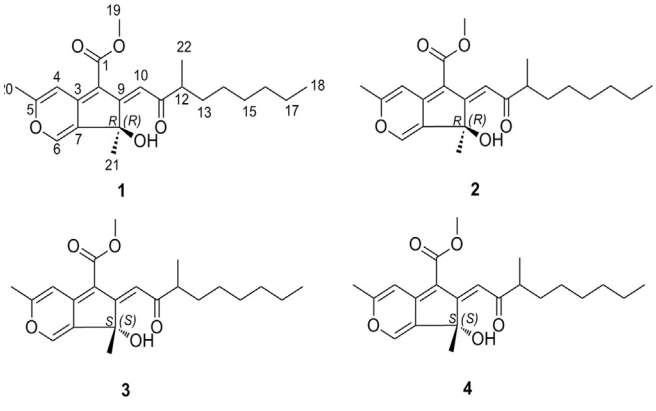

Figure 1 Chemical structures of **1**−**4**.

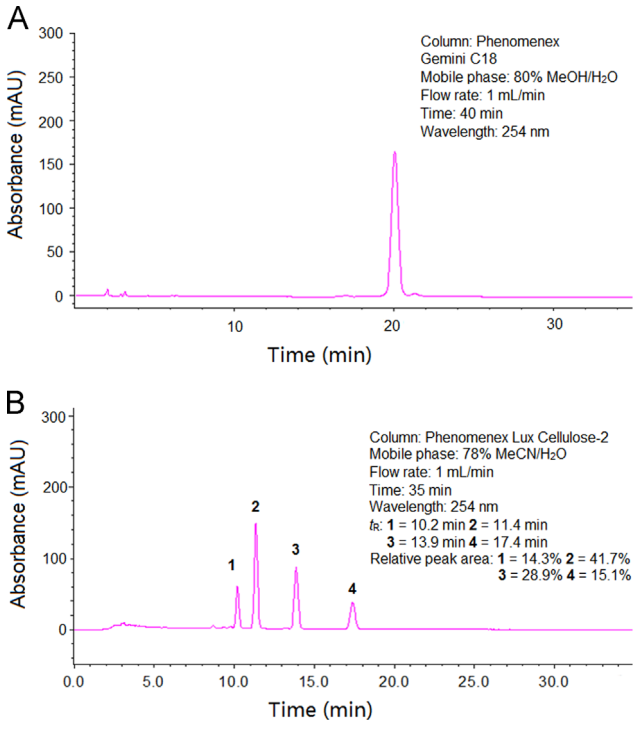

Figure 2 HPLC analysis of **1**–**4** (A: the analysis of **1**–**4** on routine ODS HPLC; B: the analysis of **1**–**4** on chiral HPLC).

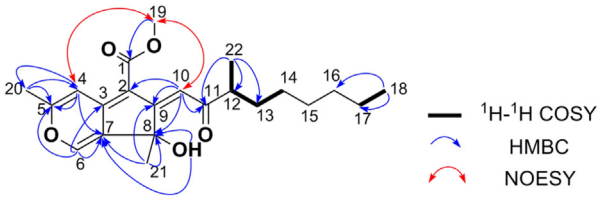

Figure 3 Key ^{1}H–^{1}H COSY, HMBC, and NOESY correlations of **1**.

3. Conclusions

Up to now, only few sequoiatones have been reported. Except the configuration of sequoiatone A had been established by X-ray crystallography[1], the absolute configurations of C-8 and C-12 in other sequoiatones were not unambiguously investigated. In our investigation, four stereoisomers of sequoiationes were isolated by chiral HPLC, whose planar structures were the same as that of sequoiatione B[1]. Among them, **1** and **3** (or **2** and **4**) are a pair of enantiomers, and **1** and **2** (or **3** and **4**) are a pair of stereoisomers with epimerization at C-12, which indicated that sequoiatione-type metabolites exist as enantiomers rather than as optically pure compounds in some strains. Based on the analyses of experimental and quantum chemical ECD, it was found that the absolute configuration of C-8 in sequoiationes can be determined by ECD, which is the first time to discuss the absolute configuration of C-8 in sequoiationes. The absolute configurations of C-12 in sequoiationes are still unsolved.

Table 1 ^{1}H NMR (400 MHz) and ^{13}C NMR (100 MHz) spectral data of **1**–**4** (δ in ppm, J in Hz, $CDCl_3$).

No.	**1**		**2**		**3**		**4**	
	δ_C	δ_H[a]	δ_C	δ_H[a]	δ_C	δ_H[a]	δ_C	δ_H[a]
1	165.4		165.4		165.4		165.4	
2	106.7		106.7		106.7		106.7	
3	152.7		152.8		152.7		152.8	
4	106.6	6.96, s	106.6	6.96, s	106.6	6.96, s	106.6	6.96, s
5	163.9		163.9		163.9		163.9	
6	141.9	7.40, s	141.9	7.41, s	141.9	7.40, s	141.9	7.41, s
7	135.4		135.4		135.4		135.4	
8	77.7		77.6		77.7		77.6	
9	168.7		168.6		168.7		168.6	
10	113.2	7.21, s	113.4	7.21, s	113.2	7.21, s	113.4	7.21, s
11	208.0		208.0		208.0		208.0	
12	47.4	2.67	47.3	2.69	47.4	2.67	47.3	2.69
13	34.0	1.68, Ha; 1.38, Hb	34.0	1.69, Ha; 1.40, Hb	34.0	1.68, Ha; 1.38, Hb	34.0	1.69, Ha; 1.39, Hb
14	27.4	1.28[b]	27.4	1.28[b]	27.4	1.28[b]	27.4	1.28[b]
15	29.4	1.28[b]	29.4	1.28[b]	29.4	1.28[b]	29.4	1.28[b]
16	31.7	1.28[b]	31.7	1.28[b]	31.7	1.28[b]	31.7	1.28[b]
17	22.6	1.25	22.6	1.25	22.6	1.25	22.6	1.25
18	14.1	0.86, t (6.8)	14.1	0.86, t (6.8)	14.1	0.86, t (6.8)	14.1	0.86, t (6.8)
19	50.9	3.84, s	50.9	3.84, s	50.9	3.84, s	50.9	3.84, s
20	20.3	2.26, s	20.4	2.26, s	20.3	2.26, s	20.4	2.26, s
21	27.3	1.53, s	27.3	1.53, s	27.3	1.53, s	27.3	1.53, s
22	17.4	1.14, d (6.9)	17.1	1.12, d (6.8)	17.4	1.14, d (6.9)	17.1	1.12, d (6.8)
OH-8		7.54, s		7.58, br s		7.53, s		7.57, br s

[a]Indiscernible signals owing to overlapping or having complex multiplicity are reported without designating multiplicity.
[b]The assignments in each column may be interchanged.

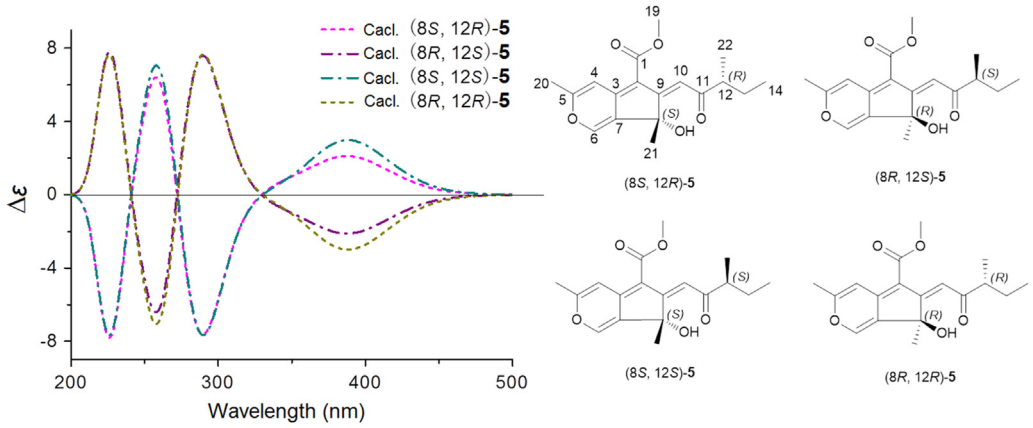

Figure 4 The calculated ECD spectra of (8*S*,12*R*)-**5**, (8*R*,12*S*)-**5**, (8*S*,12*S*)-**5**, and (8*R*,12*R*)-**5** (band width $\sigma = 0.3$ eV).

4. Experimental

4.1. General experimental procedures

Optical rotations were measured on a JASCO P1020 digital polarimeter (Jasco International Co., Ltd., Tokyo, Japan). UV data were recorded using a JASCO V-550 UV/vis spectrometer (Jasco International Co., Ltd., Tokyo, Japan). IR data were recorded on a JASCO FT/IR-480 plus spectrometer (Jasco International Co., Ltd., Tokyo, Japan). ECD spectrum was recorded on a JASCO J-810 spectrophotometer using MeOH as the solvent (Jasco International Co., Ltd., Tokyo, Japan). The ESI-MS spectra were performed on a Finnigan LCQ Advantage MAX mass spectrometer (Finnigan MAT GmbH, Bremen, Germany). The HR-ESI-MS spectra were obtained on a Micromass Q-TOF mass spectrometer (Waters Corporation, Milford, MA, USA). The NMR spectra were measured with Bruker AV-400 spectrometer (Bruker BioSpin Group, Faellanden, Switzerland) using solvent signals ($CDCl_3$: δ_H 7.26/δ_C 77.0) as internal standard. The analytical HPLC was performed on a Dionex HPLC system equipped with an Ultimate 3000 pump, an Ultimate 3000 diode array detector (DAD), an Ultimate 3000 Column Compartment, and an Ultimate 3000 autosampler (Thermo Fisher Scientific, Inc., Waltham, MA, USA) using a Phenomenex Gemini C18 column (250 mm × 4.6 mm, 5 µm) (Phenomenex Inc., Los Angeles, CA, USA). The semi-preparative HPLC was performed on a Shimadzu LC-6-AD Liquid Chromatography with an SPD-20A Detector using a Phenomenex Gemini C18 column (250 mm × 10.0 mm, 5 µm) (Phenomenex Inc., Los Angeles, CA, USA). The chiral HPLC was performed on a Shimadzu LC-6-AD Liquid Chromatography with an SPD-20A Detector using a Phenomenex Lux Cellulose-2 chiral column (250 mm × 4.6 mm, 3 µm) (Phenomenex Inc., Los Angeles, CA, USA). The medium pressure liquid chromatography (MPLC) was performed on ODS (60–80 µm, YMC Co., Ltd., Tokyo, Japan) and equipped with a dual pump gradient system, a UV preparative detector, and a Dr Flash II fraction collector system (Lisui E-Tech Co., Ltd., Shanghai, China).

4.2. Fungus material

The strain AHK07-3 was isolated from the soil, collected at the wetland of Ahongkou, Sinkiang Province, China. The strain was identified as *Talaromyces flavus* based on the morphological characters and gene sequence analysis. The ribosomal internal transcribed spacer (ITS) and the 5.8S rRNA gene sequences (ITS1-5.8S-ITS2) of the strain have been deposited at GenBank as KX011167. The fungus was cultured on slants of potato dextrose agar at 25 °C for 5 days. Agar plugs were used to inoculate four Erlenmeyer flasks (250 mL), each containing 100 mL of potato dextrose broth. Four flasks of the inoculated media were incubated at 25 °C on a rotary shaker at 200 rpm for 5 days to prepare the seed culture. Fermentation was carried out in 20 Erlenmeyer flasks (500 mL), each containing 70 g of rice. Distilled H_2O (105 mL) was added to each flask, and the rice was soaked overnight before autoclaving at 120 °C for 30 min. After cooling to room temperature, each flask was inoculated with 5.0 mL of the spore inoculum and incubated at room temperature for 50 days.

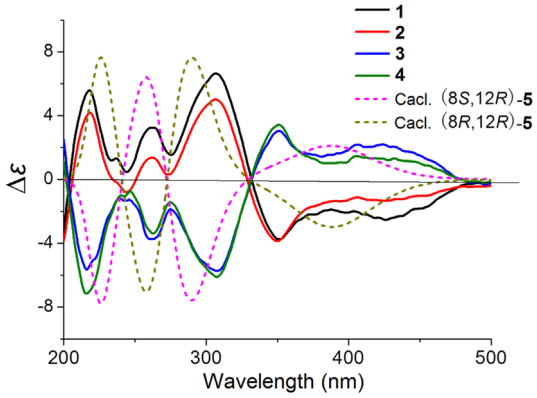

Figure 5 The experimental ECD spectra of **1**−**4** and calculated ECD spectra of (8*S*,12*R*)-**5** and (8*R*,12*R*)-**5** (UV correction = 0 nm, band width $\sigma = 0.3$ eV).

4.3. Extraction and isolation

The culture was extracted three times with EtOAc, and the organic solvent was removed under reduced pressure to yield crude extract (19.7 g). The crude extract was dissolved in 90% *v*/*v* aqueous MeOH (400 mL) and partitioned against the same volume of cyclohexane to afford a cyclohexane fraction (C, 4.6 g) and an aqueous MeOH fraction (W, 14.7 g). The aqueous MeOH fraction

(W, 14.7 g) was separated by MPLC (195 mm × 31.2 mm) eluting with MeOH − H_2O (30:70 and 100:0, *v/v*) and $CHCl_3$ − MeOH (50:50, *v/v*) to afford three fractions (W1 to W3). The fraction W2 (5.9 g) was separated by MPLC (127 mm × 26.8 mm) with a gradient of MeOH − H_2O (60% − 100%, *v/v*) to yield four subfractions (W2a to W2d). The subfraction W2c (521.8 mg) was further separated by MPLC (76 mm × 21.4 mm) with a gradient of MeOH − H_2O (60% − 90%, *v/v*) to yield three sub-subfractions (W2c1 to W2c3). Sub-subfraction W2c2 (100.6 mg) was purified by semi-preparative HPLC purification using MeOH–H_2O (73:27, *v/v*) with 0.1% formic acid at a flow rate of 3 mL/min to yield an isolated peak W2c2-3 (18.6 mg) and it was separated by chiral HPLC using MeCN–H_2O (78:22, *v/v*) at a flow rate of 1 mL/min to afford **1** (t_R: 10.2 min, 3.0 mg), **2** (t_R: 11.4 min, 4.2 mg), **3** (t_R: 13.9 min, 3.7 mg), and **4** (t_R: 17.4 min, 2.8 mg), respectively.

Compound 1 Yellow oil; $[\alpha]_D^{25}$ −109.8 (*c* 0.50, MeOH); UV (MeOH) λ_{max} (logε) 204 (3.25), 253 (3.17), 314 (3.08), 426 (3.53) nm; CD (*c* 2.1×10^{-4} mol/L, MeOH) λ_{max} ($\Delta\varepsilon$) 218 (+5.55), 262 (+3.27), 306 (+6.63), 352 (−3.75), 426 (−2.59) nm; IR (KBr) ν_{max} 3440, 2925, 1664, 1541, 1501, 1459, 1172, 1127, 1057 cm^{-1}; ^1H NMR (400 MHz, $CDCl_3$) and ^{13}C NMR (100 MHz, $CDCl_3$) see Table 1; ESI-MS (positive): *m/z* 375 $[M+H]^+$, 397 $[M+Na]^+$, HR-ESI-MS (positive): *m/z* 375.2177 $[M+H]^+$ (Calcd. for $C_{22}H_{31}O_5$, 375.2171).

Compound 2 Yellow oil; $[\alpha]_D^{25}$ −51.2 (*c* 0.50, MeOH); UV (MeOH) λ_{max} (logε) 204 (3.19), 254 (3.10), 314 (3.02), 426 (3.51) nm; CD (*c* 2.1×10^{-4} mol/L, MeOH) λ_{max} ($\Delta\varepsilon$) 218 (+4.21), 262 (+1.39), 306 (+5.06), 350 (−3.84), 426 (−1.34) nm; IR (KBr) ν_{max} 3440, 2925, 1670, 1541, 1507, 1457, 1172, 1114, 1064 cm^{-1}; ^1H NMR (400 MHz, $CDCl_3$) and ^{13}C NMR (100 MHz, $CDCl_3$) see Table 1; ESI-MS (positive): *m/z* 375 $[M+H]^+$, 397 $[M+Na]^+$, HR-ESI-MS (positive): *m/z* 375.2182 $[M+H]^+$ (Calcd. for $C_{22}H_{31}O_5$, 375.2171).

Compound 3 Yellow oil; $[\alpha]_D^{25}$ +113.8 (*c* 0.50, MeOH); UV (MeOH) λ_{max} (logε) 204 (3.27), 253 (3.17), 314 (3.08), 426 (3.53) nm; CD (*c* 2.1×10^{-4} mol/L, MeOH) λ_{max} ($\Delta\varepsilon$) 216 (−5.59), 262 (−3.75), 307 (−5.72), 351 (+3.05), 426 (+2.20) nm; IR (KBr) ν_{max} 3440, 2925, 1664, 1541, 1501, 1459, 1172, 1127, 1057 cm^{-1}; ^1H NMR (400 MHz, $CDCl_3$) and ^{13}C NMR (100 MHz, $CDCl_3$) see Table 1; ESI-MS (positive): *m/z* 375 $[M+H]^+$, 397 $[M+Na]^+$, HR-ESI-MS (positive): *m/z* 375.2177 $[M+H]^+$ (Calcd. for $C_{22}H_{31}O_5$, 375.2171).

Compound 4 Yellow oil; $[\alpha]_D^{25}$ +57.2 (*c* 0.50, MeOH); UV (MeOH) λ_{max} (logε) 204 (3.20), 254 (3.10), 314 (3.02), 426 (3.51) nm; CD (*c* 2.1×10^{-4} mol/L, MeOH) λ_{max} ($\Delta\varepsilon$) 216 (−7.11), 262 (−3.40), 307 (−6.08), 351 (+3.41), 426 (+1.30) nm; IR (KBr) ν_{max} 3440, 2925, 1670, 1541, 1507, 1457, 1172, 1114, 1064 cm^{-1}; ^1H (400 MHz, $CDCl_3$) and ^{13}C NMR (100 MHz, $CDCl_3$) see Table 1; ESI-MS (positive): *m/z* 375 $[M+H]^+$, 397 $[M+Na]^+$, HR-ESI-MS (positive): *m/z* 375.2185 $[M+H]^+$ (Calcd. for $C_{22}H_{31}O_5$, 375.2171).

4.4. ECD calculation

Before molecular initial 3D structures were generated with CORINA version 3.4, the molecules of (8*S*, 12*R*)-**5**, (8*R*, 12*S*)-**5**, (8*S*, 12*S*)-**5**, and (8*R*, 12*R*)-**5** were converted into SMILES codes, respectively. Conformer databases were generated in CONFLEX version 7.0 using the MMFF94s force-field, with an energy window for acceptable conformers (ewindow) of 5 kcal/mol above the ground state, a maximum number of conformations per molecule (maxconfs) of 100, and an RMSD cutoff (rmsd) of 0.5 Å. Then each conformer of the acceptable conformers was optimized with HF/6-31G(d) method in Gaussian09[17]. Further optimization at the APFD/6-31G(d) level led the dihedral angles to be got. After that, thirteen lowest energy conformers of (8*S*, 12*R*)-**5** and (8*R*, 12*S*)-**5** were found out (see Supplementary Information Table S5 and Fig. S1). Fourteen lowest energy conformers of (8*S*, 12*S*)-**5** and (8*R*, 12*R*)-**5** were found out (see supporting information Table S6 and Fig. S2). The optimized conformers were taken for the ECD calculations, which were performed with Gaussian09 (APFD/6-311++G(2d,p)). The solvent effect was taken into account by the polarizable-conductor calculation model (IEFPCM, methanol as the solvent). Comparisons of the experimental and calculated spectra were done with the software SpecDis[18,19]. It was also used to apply a UV shift to the ECD spectra, Gaussian broadening of the excitations, and Boltzmann weighting of the spectra.

Acknowledgments

This work was financially supported by grants from the National Natural Science Foundation of China (Nos. 81422054 and 81172945), the Guangdong Natural Science Funds for Distinguished Young Scholar (S2013050014287), Guangdong Special Support Program (2014TQ01R420), and Guangdong Province Universities and Colleges Pearl River Scholar Funded Scheme (Hao Gao, 2014).

Appendix A. Supplementary material

Supplementary data associated with this article can be found in the online version at http:dx.doi.org/10.1016/j.apsb.2016.07.005.

References

1. Stierle AA, Stierle DB, Bugni T. Sequoiatones A and B: novel antitumor metabolites isolated from a redwood endophyte. *J Org Chem* 1999;**64**:5479–84.
2. Stierle AA, Stierle DB, Bugni T. Sequoiatones C-F, constituents of the redwood endophyte *Aspergillus parasiticus*. *J Nat Prod* 2001;**64**:1350–3.
3. Lin ZJ, Zhu TJ, Fang YC, Gu QQ, Zhu WM. Polyketides from *Penicillium* sp. JP-1, an endophytic fungus associated with the mangrove plant *Aegiceras corniculatum*. *Phytochemistry* 2008;**69**:1273–8.
4. Fielding BC, Haws EJ, Holker JSE, Powell ADG, Robertson A, Stanway DN, et al. Monascorubrin. *Tetrahedron Lett* 1960;**1**:24–7.
5. Steyn PS, Vleggaar R. A reinvestigation of the structure of monochaetin, a metabolite of *Monochaetia compta*. *J Chem Soc Perkin Trans 1* 1986;**1986**:1975–6.
6. He JW, Mu ZQ, Gao H, Chen GD, Zhao Q, Hu D, et al. New polyesters from *Talaromyces flavus*. *Tetrahedron* 2014;**70**:4425–30.
7. He JW, Qin DP, Gao H, Kuang RQ, Yu Y, Liu XZ, et al. Two new coumarins from *Talaromyces flavus*. *Molecules* 2014;**19**:20880–7.
8. He JW, Liang HX, Gao H, Kuang RQ, Chen GD, Hu D, et al. Talaflavuterpenoid A, a new nardosinane-type sesquiterpene from *Talaromyces flavus*. *J Asian Nat Prod Res* 2014;**16**:1029–34.
9. Bao YR, Chen GD, Wu YH, Li XX, Hu D, Liu XZ, et al. Stachybisbins A and B, the first cases of seco-bisabosquals from *Stachybotrys bisbyi*. *Fitoterapia* 2015;**105**:151–5.
10. Bao YR, Chen GD, Gao H, He RR, Wu YH, Li XX, et al. 4, 5-*seco*-probotryenols A-C, a new type of sesquiterpenoids from *Stachybotrys bisbyi*. *RSC Adv* 2015;**5**:46252–9.

11. Wang CX, Chen GD, Feng CC, He RR, Qin SY, Hu D, et al. Same data, different structures: diastereoisomers with substantially identical NMR data from nature. *Chem Commun* 2016;**52**:1250–3.
12. Ren JW, Zhang F, Liu XY, Li L, Liu G, Liu XZ, et al. Neonectrolide A, a new oxaphenalenone spiroketal from the fungus *Neonectria* sp. *Org Lett* 2012;**14**:6226–9.
13. Li L, Li C, Si YK, Yin DL. Absolute configuration of buagafuran: an experimental and theoretical electronic circular dichroism study. *Chin Chem Lett* 2013;**24**:500–2.
14. Wu ZY, Wu Y, Chen GD, Hu D, Li XX, Sun X, et al. Xylariterpenoids A–D, four new sesquiterpenoids from the Xylariaceae fungus. *RSC Adv* 2014;**4**:54144–8.
15. Jia YL, Wei MY, Chen HY, Guan FF, Wang CY, Shao CL. (+)- and (−)-Pestaloxazine A, a pair of antiviral enantiomeric alkaloid dimers with a symmetric spiro[oxazinane-piperazinedione] skeleton from *Pestalotiopsis* sp. *Org Lett* 2015;**17**:4216–9.
16. Chen GD, Xiao GK, Yao XS, Gao H. Electronic circular dichroism calculation method in the assignment of absolute configuration of natural products. *J Int Pharm Res* 2015;**42**:738–43.
17. Frisch MJ, Trucks GW, Schlegel HB, Scuseria GE, Robb MA, Cheeseman JR, et al. *Gaussian 09, revision D.01*. Wallingford CT: Gaussian, Inc; 2010.
18. Bruhn T, Schaumlöffel A, Hemberger Y, Bringmann G. *SpecDis, version 1.61*. Würzburg, Germany: University of Würzburg; 2013.
19. Bruhn T, Schaumlöffel A, Hemberger Y, Bringmann G. SpecDis: quantifying the comparison of calculated and experimental electronic circular dichroism spectra. *Chirality* 2013;**25**:243–9.